Clay Swelling and Formation Permeability Reductions Induced by a Nonionic Surfactant

KEVIN H. GARDNER* AND
MIGUEL S. ARIAS

Department of Civil Engineering, University of New Hampshire, Durham, New Hampshire 03824

A major concern with the use of surfactant flushing to mobilize nonaqueous phase liquids in aquifers is specific mineral−surfactant interactions that may effect significant permeability changes in the soil formation. Soils comprised of Ottawa sand mixed with small percentages of bentonite ($0-5\%$) that had moderate initial hydraulic conductivity ($>10^{-6}$ m/s) were investigated for loss of permeability upon flushing with solution containing a nonionic surfactant (polyoxyethylene sorbitan monooleate). Columns containing 0, 1, 2, 3, 4, and 5% clay had permeability reductions of 1, 5, 13, 44, 49, and 69%, respectively. The surfactant−clay interactions were further investigated as the cause of the permeability reductions. Some transport of clay through the column was apparent from a small amount of release measured. A permeability change was correlated with the colloid transport in the column with the highest clay concentration, although its effect was transient. Clay swelling was postulated as the primary mechanism for the permeability reductions. It was determined through X-ray diffraction that the surfactant was spreading the silica layer spacings of the clay from a hydration spacing of 15.23 Å to a surfactant-swelled spacing of 18.02 Å. A model was formulated to describe the reduced permeability by the increase in clay volume due to swelling measured by X-ray diffraction and was capable of describing the observed data well with an average error of approximately 10%.

Introduction

An emerging remediation technique to restore aquifers contaminated by nonaqueous phase liquid (NAPL) is the addition of a surface-active agent (surfactant) to soil flushing water. There have been several successful laboratory and field surfactant soil flushing tests performed, and appropriate descriptions of the resulting miscibility and mobility behavior have emerged (*1−21*).

A few studies have also shown, however, that surfactants may induce physical changes in the aquifer that can change the hydraulic conductivity and permeability of the medium. Allred and Brown (*22*), for example, reported a permeability reduction of 2 orders of magnitude after surfactant injection into a fine-grained soil. Renshaw et al. (*23*) demonstrated permeability reductions in clay soils and attributed the phenomenon to decreased pore area as a result of surfactant sorption. Pennell and co-workers (*5*) cited the migration of fines as the source of hydraulic conductivity loss in dodecane-

* Corresponding author e-mail: kevin.gardner@unh.edu; phone: (603)862-4334; fax: (603)862-3957.

contaminated sand treated with a nonionic surfactant, while surfactant-induced flocculation and channeling was cited by Meegoda and Rajapakse (*24*) as the cause of an observed hydraulic conductivity increase of up to 3 orders of magnitude in clays. Tumeo (*25*) provided a comprehensive literature review of hypotheses related to hydraulic conductivity change.

The mechanisms by which these changes occur remain largely unresolved but are important to decipher if this type of remediation is to be robust. Unexpected changes in hydraulic conductivity during remedial operations can have significant effects. Decreases in hydraulic conductivity may result in a more costly operation or may render the treatment unfeasible. Increases in hydraulic conductivity may result in further spreading of the contaminant plume beyond the hydraulic controls that are in place. Overall, there are very few studies directly related to the effect of surfactants on either permeability or hydraulic conductivity. As a result, there is still great uncertainty associated with how and when hydraulic conductivity will be affected by surfactant addition. The mechanisms by which these changes occur were the focus of the research reported here. Specifically, this paper presents the results of a mechanistic investigation of permeability loss in artificial soils that would meet standard screening criteria for remediation by surfactant flushing [hydraulic conductivity greater than $\sim 10^{-6}$ m/s (*9*)]. The soils contained small concentrations of a swelling clay ($0-5\%$) and were subjected to flushing with a commonly used nonionic surfactant, polyoxyethylene sorbitan monooleate.

Laboratory Materials and Methods

To quantify surfactant-induced permeability changes, a series of experiments were performed on sand−clay columns. Constant head tests were used to allow the experiment to continue while measurements of hydraulic conductivity were made.

Polyoxyethylene sorbitan monooleate (POE SM) is a nonionic surfactant that was used in all experimentation. POE SM is a promising surfactant for the remediation of NAPL-contaminated groundwaters as demonstrated by previous research (cf. ref *5*) and because of its food additive status. POE SM was used as received (Sigma-Aldrich). Average molecular weight and density of POE SM are 1310 g/mol and 1.08 g/mL, respectively, and the critical micelle concentration (cmc) is 13 mg/L (*5*). Influent solutions in the column experiments contained 2.6 g/L or 200 times the cmc of POE SM in a background electrolyte concentration of 10^{-3} M NaCl, as suggested by previous research (*5, 26*). It was determined that the electrolyte−POE SM solution had a viscosity of 1.0580×10^{-2} g cm^{-1} s^{-1} and a density of 0.9875 g/mL at a temperature of 20 °C. All of the solutions were prepared with deionized water that passed through a Barnstead Nanopure water filtration system.

Ottawa sand was selected as the porous medium for the column experiments because it is a nonporous silica sand and has a limited sorption capacity for surfactant. The surface area of the Ottawa sand was 0.025 m²/g as determined by N₂ BET adsorption; the particle size was normally distributed with a median of 130 μm, as determined using a Coulter LS-230; and the hydraulic conductivity was 3.34×10^{-3} cm/s as determined using the apparatus described below. The sand was washed with 10^{-2} M HCl, rinsed, and dried prior to use. Bentonite clay (Archer Daniels Midland Company) was selected as a representative swelling clay because it is often found in hydrogeologic units and strongly sorbs many common surfactants (*23*).

Bentonite clay (0−5 wt %) was mixed with Ottawa sand until homogenized and packed into glass columns. Columns had an inner diameter of 2.5 cm and a length of 7.5 cm (Fischer and Porter Company, Warminster, PA.). The columns were capped with a porous stone at each end. The porous stones were approximately 5 mm in thickness and did not retain any bentonite clay that was dispersed in the flow field.

A constant head was placed on the column with a hydraulic gradient of approximately 20 (a high gradient was used to limit the time scale of experiments where permeability became low). Two constant head reservoirs were used. One reservoir contained a background electrolyte solution (10^{-3} NaCl), and the other contained the surfactant (2.6 g/L POE SM) in addition to the electrolyte. Initially, electrolyte solution only was passed through the column. Flow was monitored periodically for 30−35 pore volumes of electrolyte to ensure that the flow rate had reached steady state. After stabilization of the column, several additional pore volumes of electrolyte were passed through the column to obtain initial permeability measurements. Column effluent was collected in graduated test tubes with a fraction collector, and permeability was determined by measuring flow rate through the column at discrete time intervals. Permeability was calculated from flow rate by

$$k = \frac{QL\mu}{Ah\rho g} \qquad (1)$$

where k is the permeability of the medium (L²), Q is the flow rate through the column (L³/T), L is the length of the packed bed (L), μ is the fluid viscosity (M/LT), A is the column's cross-sectional area (L²), h is the head of water (L), ρ is the fluid density (M/L³), and g is the gravitational constant (L/T²).

With the initial permeability measurements taken, influent was switched to surfactant, and changes in permeability were monitored over time. The concentration of the surfactant in the column effluent was determined using a Milton Roy Spectronic 20D UV spectrophotometer at a wavelength of 565 nm.

Results and Discussion

The surfactant-induced changes in permeability were first investigated using columns containing only Ottawa sand. It was necessary to quantify permeability changes in the sand, enabling tests to be performed on sand−clay columns where any differences in the permeability changes could be attributed to the clay fraction. Figure 1a shows the permeability (k) of Ottawa sand exposed to POE SM normalized to the initial permeability when the column is stabilized with electrolyte (k_0). Also shown is the effluent concentration of POE SM (C), normalized to the influent surfactant concentration (C_0). The pure sand column had a minimal decrease in permeability with the surfactant breakthrough (∼98−99% of initial permeability). The midpoint of the breakthrough curve occurred at 1.05 pore volumes after surfactant solution was introduced. This minor retardation of the breakthrough curve is likely due to limited sorption of POE SM onto the Ottawa sand. The concentration of adsorbed sorbitan monooleate estimated from the breakthrough curve is 0.03 $mg_{surfactant}/g_{sand}$.

Adsorption isotherms were performed using a standard batch approach and the sorption capacity for the Ottawa sand was found to be 2.23 $mg_{surfactant}/g_{sand}$. This is similar to that found by Pennell et al. (5), who determined the sorption capacity to be 1.33 mg/g. For the experimental conditions of Figure 1 (influent surfactant concentration of 2.6 g/L), the Langmuir isotherm predicts a sorption capacity of 0.86 mg/g, which is significantly higher than the estimate obtained from the retardation of the breakthrough curve (0.03 mg/g).

This may be due to the kinetics of the sorption reaction and, secondarily, may be attributable to the loss of available surface area when sand is packed into the column (27). The adsorption of surfactant is a possible mechanism for the small permeability reduction that was observed, as has been postulated by others (23).

Figure 1b shows that the column containing 3% clay reaches a steady-state permeability of 56% of the initial permeability and that the breakthrough curve is slightly retarded (1.87 pore volumes until $C/C_0 = 0.5$), due mostly to the clay in the system that sorbs surfactant to a greater extent than the sand. Estimating the sorption capacity of the bentonite in the column (using the breakthrough curve and neglecting the surfactant sorbed by the sand) yields a value of 18.6 $mg_{surfactant}/g_{clay}$. Adsorption isotherms were also developed for adsorption of POE SM on bentonite clay, and fitting the Langmuir isotherm yields a sorption capacity of 114 mg/g. The equilibrium sorption at 2.6 g/L of surfactant is 64.6 mg/g, which is approximately three times that observed in column experiments. This value agrees well with previous research that indicates packing typically results in a reduction in available surface area in packed bed systems as compared with dispersions (27). It remains possible that there were kinetic limitations in this case as well, although the slower flow rate may be responsible for the closer agreement between breakthrough retardation and batch experiments (29% here vs 3.5% for the Ottawa sand column above).

Also noticeable in Figure 1b is an apparent increase in the effluent POE SM concentration over the influent concentration, an observation that is attributable to the release of clay from the domain. The spectrophotometric measurement of surfactant is complicated by the presence of colloidal material resulting in this apparent increase. This release of colloids decreases with time, and within approximately 15 pore volumes the apparent surfactant concentration returns to the influent concentration.

Figure 2a depicts the permeability changes from all of the clay percentages (0, 1, 2, 3, 4, and 5%). The permeability for columns containing 1, 2, 3, 4, and 5% bentonite were 95, 87, 56, 51, and 31% of initial permeability, respectively, after equilibration with surfactant. There was a much greater magnitude of permeability decrease observed as clay content increased, indicating that clay content is directly related to surfactant-induced permeability changes.

Switching the effluent back to electrolyte did not give a significant recovery of permeability for any of the columns that contained clay, even after several pore volumes of electrolyte were passed through. Table 1 shows the steady-state permeability of each column initially, in equilibrium with surfactant, and when influent is switched back to electrolyte. It is evident from these results that surfactant-induced physical changes in permeability are not reversible on the near field time-scale relevant to surfactant flushing remediation. This conclusion is supported by batch desorption experiments, which indicated that sorption to clay was irreversible on a short time scale (48 h) under these particular conditions (20 °C and 10^{-3} M NaCl).

The columns containing 3, 4, and 5% clay saw much greater releases of colloidal material as shown in Figure 2b. The peaks were well above the influent concentration of surfactant, and they did not decline as rapidly as the other columns. For the apparent concentration to return to influent levels, it took approximately 15, 20, and 30 pore volumes for the 3, 4, and 5% clay columns, respectively. Effluent was collected from these columns and filtered to determine gravimetrically the amount of clay being released for the 3% and the 5% bentonite columns. This was found to be 0.05 and 0.1 g, respectively. Comparing these numbers to the clay content in the column indicates that 2.6% of the total mass of clay was released from the 5% column and 2.2% was
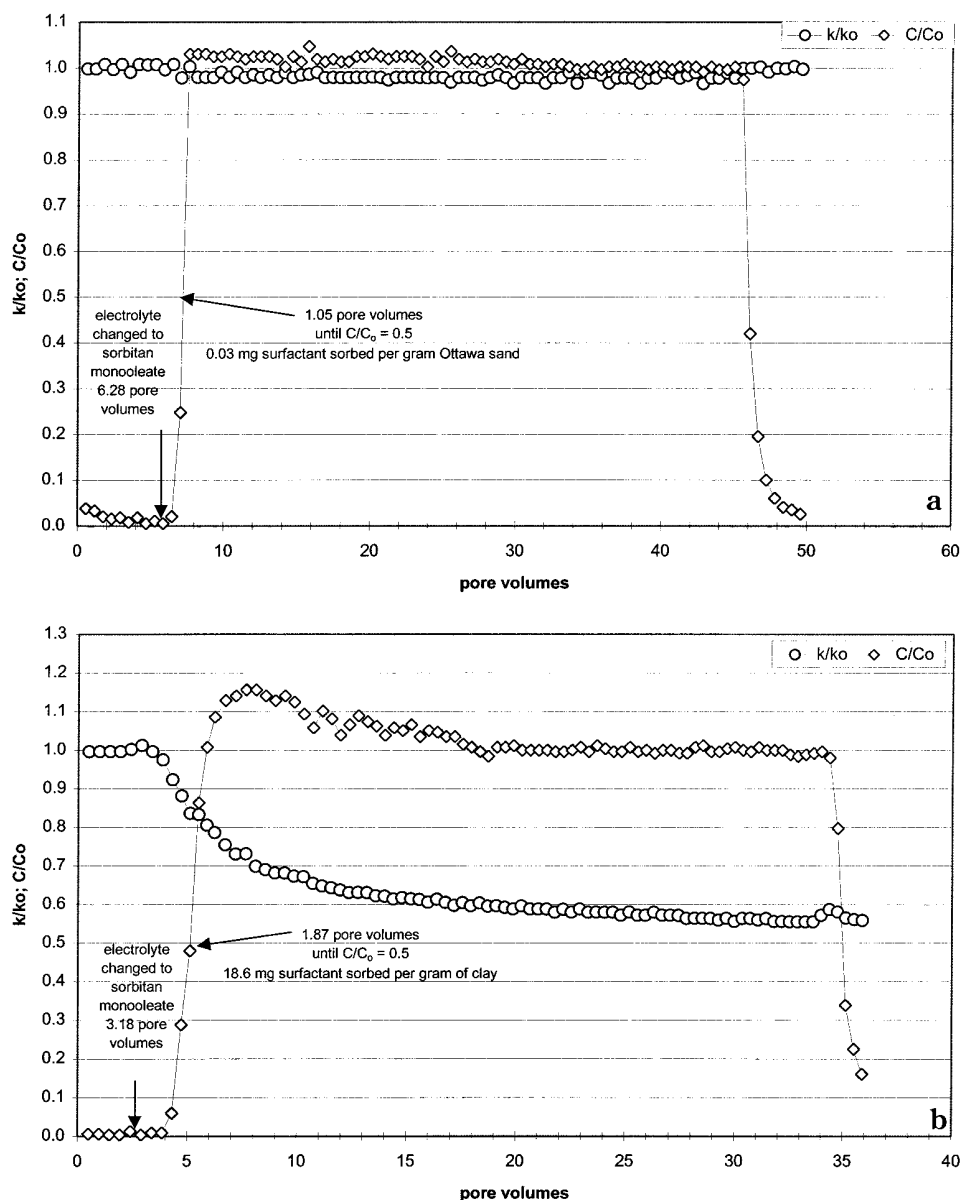
FIGURE 1. Surfactant breakthrough and permeability behavior. (a) Pure Ottawa sand. (b) 3% bentonite clay.

released from the 3% column, demonstrating that most of the clay does remain in the column. The only column to apparently be significantly affected by transport and rearrangement of colloids was the 5% clay column. It showed a decrease in permeability to 21% of the original value and, after the release of fines had subsided, a subsequent increase to 31% of the initial permeability. This indicates that the release of fines seen in this larger percentage bentonite column did have a noticeable effect on permeability but was transient in nature. Although the other columns also released fines, the same response of the permeability was not observed.

It is possible that there is more than one mechanism responsible for the permeability reductions seen in these experiments. There are two main postulates of why the permeability reductions occur:

(i) The release and redeposition of clay colloids that results in constriction of pores.

(ii) Swelling of the clay, resulting in pore size reduction.

Release/Rearrangement of Clay Colloids. It is clear that there is some rearrangement of the clay structure because

some fraction of the clay does escape into the effluent. It is possible that particles are released from the whole length of the column and do not redeposit. These particles may be a small percentage (i.e., 2.5%) of the clay in the column that became dispersed by the significant change in interfacial forces caused by surfactant adsorption. Another plausible scenario is that a much larger fraction of the clay particles were dispersed throughout the column length. Those in the upper portions of the column had sufficient contact time in the bed to redeposit, while those dispersed near the end of the column were released due to insufficient contact time. The fines seen in the effluent could be from the bottom portion of the column where the release of particles would not have sufficient contact time to reattach to the medium. In any case, it is known that most of the clay present stays in the column and that the effect on permeability from the fines redistribution appears to be transient.

Swelling of the Clay. Swelling causes the volume of pore space to be reduced due to confining forces that do not allow global deformation. Since the columns used had fixed walls,
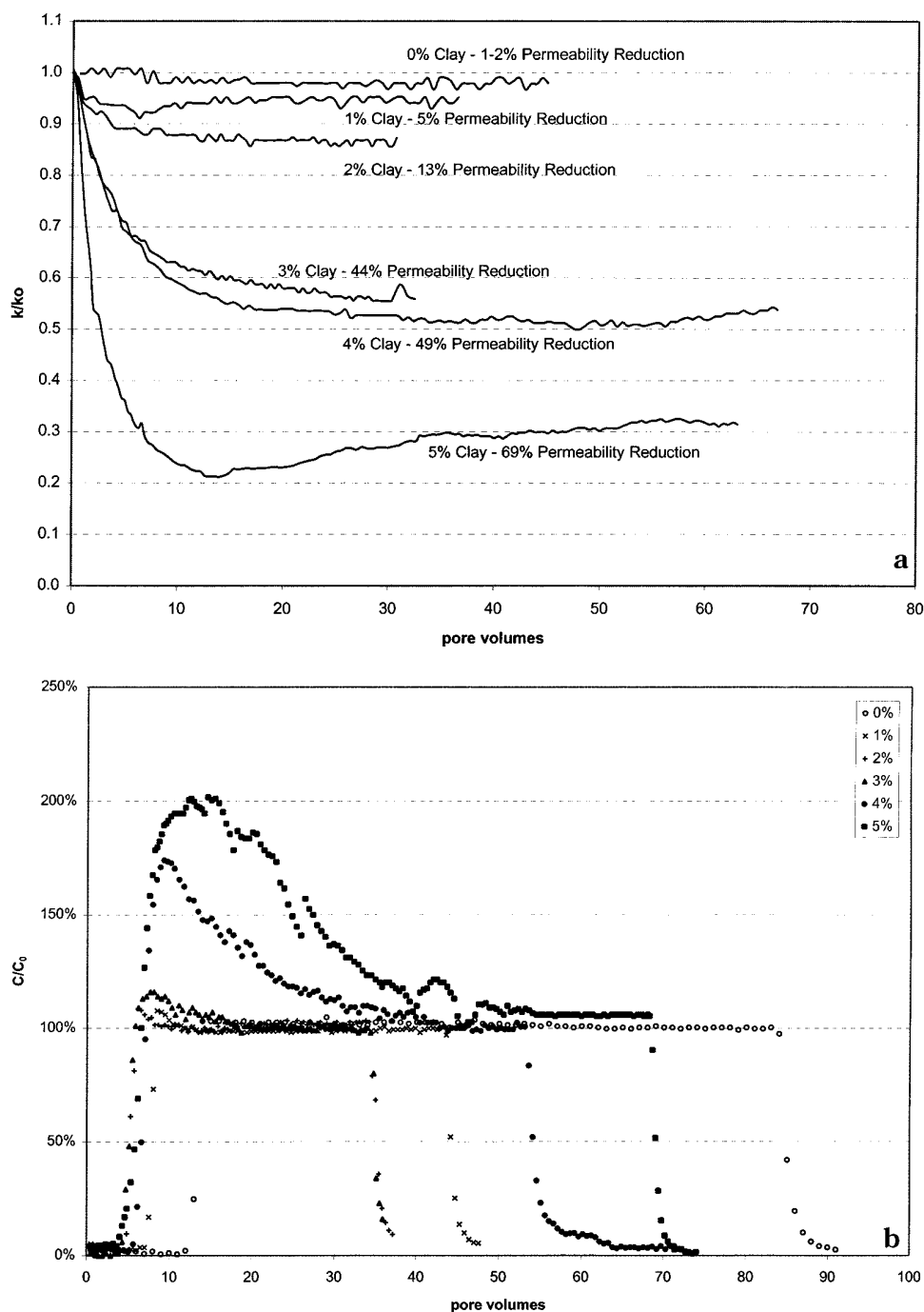
FIGURE 2. (a) Permeability changes over time for various clay contents. (b) Corresponding surfactant breakthrough behavior.

any change in the effective clay volume would correspond to a net reduction in the available pore space. Further experimentation was conducted on the clay to quantify the swelling that occurs when clay is contacted with POE SM.

X-ray diffraction was used to investigate the effects of different solutions on the interlayer silica spacings of the bentonite clay. Samples of bentonite were solvated in various solutions, air-dried on glass slides, and analyzed (Philips XRG 3100 X-ray diffractometer). Shown in Figure 3 are the peak patterns for bentonite suspended in background electrolyte and in electrolyte with 2.6 g/L POE SM. The peaks shown are a function of twice the incident angle (2Θ) of the X-rays. Figure 3 shows the bentonite solvated in background electrolyte gives a peak at 5.8° and a corresponding spacing of 15.23 Å, which is close to the spacing of 15.5 Å expected

TABLE 1. Equilibrium Permeability Changes

clay content (%)	initial k (cm²)	k in equilibrium with surfactant (cm²)	k/k_0 in equilibrium with surfactant (%)	k/k_0 in equilibrium with electrolyte[a] (%)
0	3.44×10^{-8}	3.37×10^{-8}	99	100
1	2.12×10^{-8}	2.01×10^{-8}	95	95
2	1.43×10^{-8}	1.24×10^{-8}	87	89
3	5.83×10^{-9}	3.26×10^{-9}	56	56
4	2.47×10^{-9}	1.26×10^{-9}	51	52
5	1.08×10^{-9}	3.35×10^{-10}	31	34

[a] Values represent k/k_0 after equilibration with surfactant and subsequent flushing with electrolyte solution in the absence of surfactant.

TABLE 2. Change in Column Parameters and Permeability Reduction Model Predictions

% bentonite	initial porosity (η_0)	change in vol of clay (mL)	porosity (η)	biovolume ratio (α)	Ives and Pienvichitr (28) model k/k_0	Tien et al. (31) model k/k_0	measured k/k_0
0	0.336	0	0.336	0.000	1.000	1.000	0.99
1	0.332	0.093	0.330	0.006	0.982	0.979	0.95
2	0.385	0.192	0.381	0.011	0.969	0.960	0.87
3	0.392	0.288	0.386	0.015	0.954	0.942	0.56
4	0.335	0.393	0.327	0.025	0.928	0.912	0.51
5	0.385	0.476	0.375	0.026	0.924	0.904	0.31
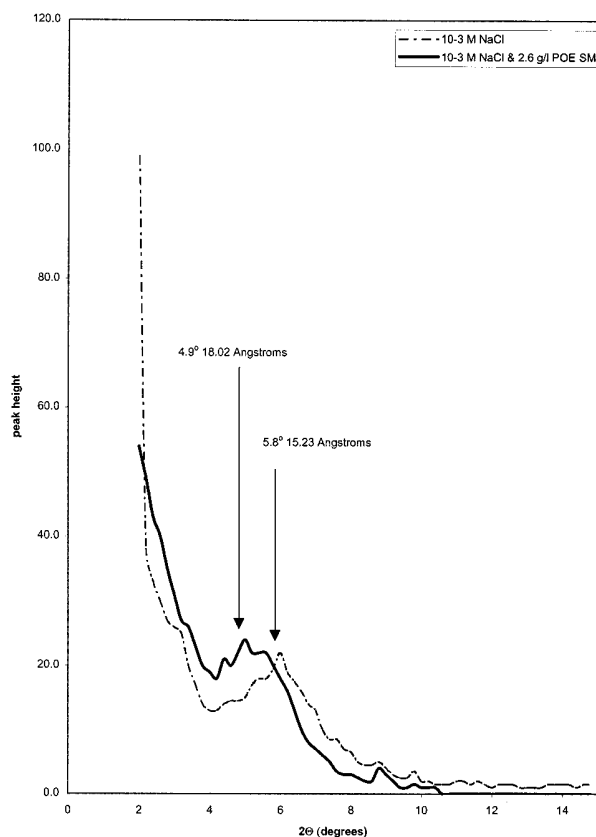
FIGURE 3. X-ray diffraction spectra for bentonite solvated in 10^{-3} M NaCl and 10^{-3} M NaCl with 2.6 g/L POE SM.

for montmorillonite dried at room temperature and moderate humidity (28).

A peak shift corresponding to a change in the spacing between silica layers was observed for clay solvated in POE SM, as shown in Figure 3. The shift due to POE SM also spreads the peak over a larger range of silica layer spacings, which indicates that the surfactant molecule may be oriented between silica layers in different positions, thus spreading the silica sheets to different separation distances. The spacing change in the clay layers is approximately 3 Å, from a hydrated spacing of 15.23 to 18.02 Å. It is postulated that this physical change in the silica spacing is the primary factor that decreases the permeability of the medium.

Permeability Reduction Models. The initial approach taken to the mathematical description of the observed phenomena was to equate the swelling of a clay crystallite to the growth of a biofilm on the clay particle. Following this, a model developed to predict permeability reduction for particle deposition in a granular media filter was assessed. Due to the poor performance of these approaches, a unique model was developed to describe the data presented here.

The Ives and Pienvichitr (29) model for permeability reductions due to biofilm growth can be expressed as follows:

$$\frac{k}{k_0} = (1 - \alpha)^{3-2P} \qquad (2)$$

where α is termed the "biovolume ratio" and is defined as $[(\eta_0 - \eta)/\eta_0]$ (dimensionless), η is the porosity of the medium after some growth has occurred (dimensionless), the subscript "0" denotes the initial value associated with the unclogged porous medium, and P is a parameter to account for capillaries that are tortuous and/or of varying radius.

Vandevivere et al. (30) compared several biofilm growth and filtration models and concluded that all of the models underestimated the reduction of permeability. Thus, for the purposes of this mathematical formulation, the parameter P was assumed to be zero, for this gives the largest possible decrease in permeability.

To determine the initial porosity, the volume of water in the hydrated clay was calculated and excluded from the initial pore volume (31). It is assumed that the particle shape of a bentonite unit plate is square, with length and width measurements of 1 μm and a thickness of 7.9 Å. The unit weight (calculated by using the mineral structure) of the bentonite is 2.74 g/cm^3. Using the experimental results obtained through X-ray diffraction, it can be seen that the equilibrium spacing of the bentonite plates in the electrolyte solution is 15.23 Å. It was assumed that this spacing occurs in both the inter- and intraparticle layers. The bentonite unit weight and particle size were used to calculate particle volume (7.9×10^{-14} cm^3), and together with the hydrated particle spacings, the unit weight for the hydrated clay was calculated to be 1.26 g/cm^3. The total mass of clay in the column was divided by this unit weight to determine the volume of hydrated clay in the porous medium. With an individual particle volume known, the total number of particles was obtained. This method also gave the volume of water in the interlayer spaces. Knowing the column dimensions (which give a column volume of 47.4 mL) and excluding the volume of water causing hydration, the initial porosity is calculated for each column. Table 2 shows the results of the porosity calculations.

This mathematical model treats clay as the fraction of the media that is growing, in that the interlayer distances are increasing due to the surfactant sorbing between sheets. Using the unit bentonite particle volume and the equilibrium surfactant spacing between silica sheets (determined to be 18.02 Å through X-ray diffraction), the increase in clay volume was determined. The clay is assumed to be both swelled at the inter- and intraparticle layers, giving an increase in clay volume of 15%. From these calculations, the final porosity (η) is determined for each column (see Table 2). Having determined the initial porosity and the change in porosity, the theoretical permeability reduction was then calculated, which is also given in Table 2. It can be seen from the table that the biofilm growth model does not describe the observed permeability reduction well.
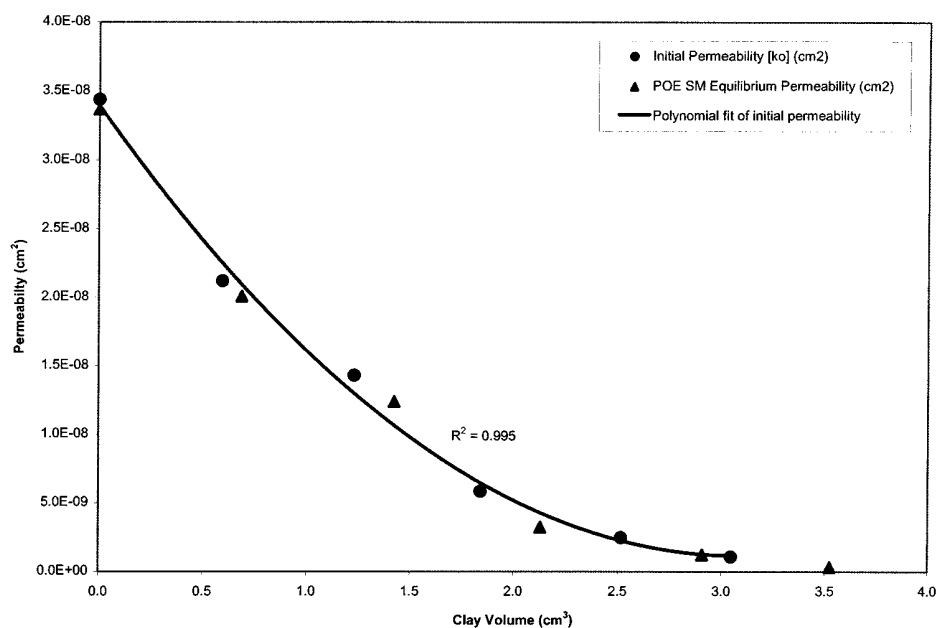
FIGURE 4. Permeability as a function of clay volume in the sample. Initial permeability is that upon exposure only to background electrolyte solution, and the polynomial is fit to these data. POE SM permeability is the measured permeability after equilibrating with the surfactant solution plotted against the volume of clay after swelling.

TABLE 3. Predicted Permeability by Basal Spacing Measurement

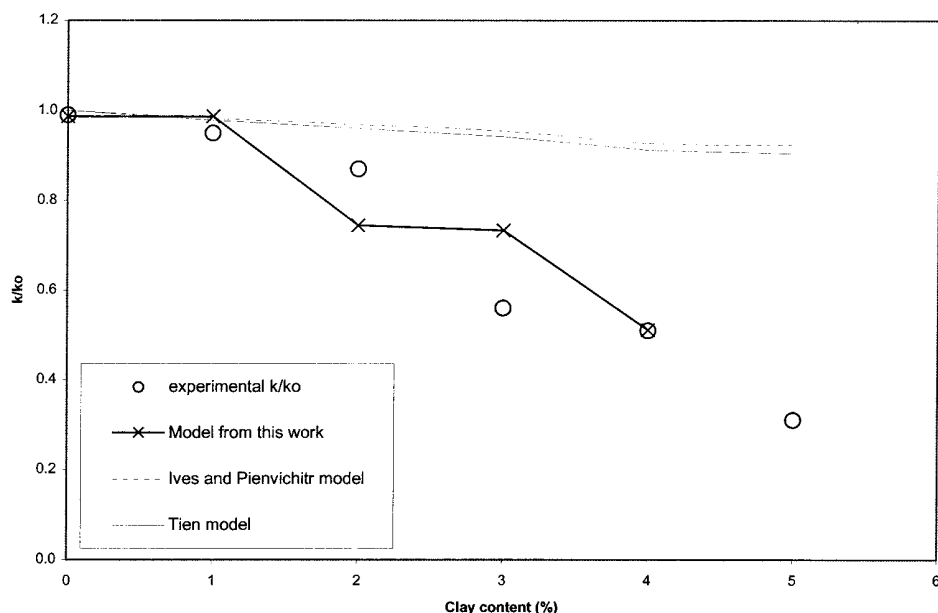| clay (%)	vol of hydrated clay (cm³)	surfactant expanded vol of clay (cm³)	initial permeability (k_0) (cm²)	predicted permeability (cm²)	measured permeability (cm²)	error (%)
0	0.00	0.00	3.44E−08	3.39E−08	3.37E−08	0.7
1	0.60	0.69	2.12E−08	2.09E−08	2.01E−08	4.1
2	1.23	1.42	1.43E−08	1.06E−08	1.24E−08	14.2
3	1.84	2.13	5.83E−09	4.28E−09	3.26E−09	31.2
4	2.52	2.91	2.47E−09	1.26E−09	1.26E−09	0.2
5	3.05	3.52	1.08E−09		3.35E−10	

FIGURE 5. Comparison of the various permeability reduction models. The model developed in this work is dependent upon data measured at higher clay contents and thus is unable to predict permeability reduction for the 5% clay column.

Due to the poor performance of the biofilm growth model, a filtration model by Tien et al. (32) was investigated. Tien's model extends the cylindrical tube model of Ives and Pienvichitr to describe the permeability reductions of filters due to the deposition of particles. Thus, the expansion of clay particles is assumed to be similar to the deposition of

particles in a granular media filter. The model is expressed as follows:

$$\frac{k}{k_0} = (1 - \alpha)^3 \left(1 + \frac{\eta_0\alpha}{1 - \eta_0}\right)^{-4/3} \qquad (3)$$

This model, however, also underpredicts the permeability reduction encountered in the columns (see Table 2).

Due to the failure encountered with the biofilm growth and filtration models, another approach was used to describe the permeability reductions. In this approach, swelled clay was considered analogous to soil with a higher clay content. In other words, it was desired to test the hypothesis that, if a soil is manufactured using sand and 1.0 cm³ of clay and this clay swells 15%, this would be equivalent to producing a soil comprised of sand with 1.15 cm³ of unswelled clay. To investigate the validity of this approach, all of the measured initial permeabilities (those that had not yet contacted surfactant) were plotted against clay volume in the soil sample. To allow for interpolation of swelled clay volumes that fall between data points, a second-order polynomial was fit to the data and is shown in Figure 4. Finally, the volume of clay in the samples after contacting surfactant and swelling was calculated. On the basis of this clay volume, new permeabilities were predicted using Figure 4. The results of this exercise are shown numerically in Table 3, along with the error between this predicted permeability and the measured, post-swelling permeability. The close agreement between these two indicates that the hypothesis is valid; that indeed swelled clay can be considered analogous to soil with a higher (unswelled) clay content. A comparison of the three permeability reduction models is shown in Figure 5. Note that the model developed here is not truly predictive as it relies on the relationship between clay content and permeability and, thus, cannot be used to extrapolate to higher clay contents without some initial permeability measurements. Rather, this model was developed and used to investigate the above hypothesis and indicates with confidence that the hypothesis is accurate for the range of experimental conditions investigated.

Acknowledgments

Literature Cited

(1) Ellis, W. D.; Payne, J. R.; McNabb, G. D. Treatment of Contaminated Soils with Aqueous Surfactants; EPA Project Summary EPA/600/S2-85/129; U.S. EPA Hazardous Waste Engineering Research Laboratory: Cincinnati, OH, 1985.

(2) Ang, C. C.; Abdul, A. S. Ground Water Monit. Rev. 1991, 11 (2), 121−127.

(3) Harwell, J. H. Factors Affecting Surfactant Performance in Groundwater Remediation Applications. In Transport and Remediation of Subsurface Contaminants; Sabatini, D. A., Knox, R. C., Eds.; ACS Symposium Series 491; American Chemical Society: Washington, DC, 1992: pp 124−132.

(4) Abdul A. S.; Gibson, T. L.; Ang, C. C.; Smith, J. C.; Sobczynski, R. E. Ground Water 1992, 30 (2), 219−231.

(5) Pennell, K. D.; Abriola, L. M.; Weber, W. J., Jr. Environ. Sci. Technol. 1993, 27 (12), 2332−2340.

(6) Brown, C. L.; Pope, G. A.; Abriola, L. M.; Sepehrnoori, K. Water Resour. Res. 1994, 30 (11), 2959−2977.

(7) Tumeo, M. A.; Braddock, J. F.; Venator, T.; Rog, S.; Owens, D. Spill Sci. Technol. Bull. 1994, 1 (1), 53−59.

(8) Pennell, K. D.; Pope, G. A.; Abriola, L. M. Environ. Sci. Technol. 1996, 30 (4), 1328−1335.

(9) Fountain, J. C.; Starr, R. C.; Middleton, T.; Beikirch, M.; Taylor, C.; Hodge, D. Ground Water 1996, 34 (5), 910−916.

(10) Okuda, I.; McBride, J. F.; Gleyzer, S. N.; Miller, C. T. Environ. Sci. Technol. 1996, 30 (6), 1852−1860.

(11) Yeom, I. T.; Ghosh, M. M.; Cox, C. D. Environ. Sci. Technol. 1996, 30 (5), 1589−1595.

(12) Hayworth, J. S.; Burris, D. R. Environ. Sci. Technol. 1997, 31 (5), 1277−1283.

(13) Hayworth, J. S.; Burris, D. R. Environ. Sci. Technol. 1997, 31 (5), 1284−1289.

(14) Roy, D., Kommalapati, R. R.; Mandava, S. S.; Valsaraj, K. T.; Constant, W. D. Environ. Sci. Technol. 1997, 31 (3), 670−675.

(15) Pennell, K. D.; Adinolfi, A. M.; Abriola, L. M.; Diallo, M. S. Environ. Sci. Technol. 1997, 31 (5), 1382−1389.

(16) Tiehm, A.; Stieber, M.; Werner, P.; Frimmel, F. H. Environ. Sci. Technol. 1997, 31 (9), 2570−2576.

(17) Smith, J. A.; Sahoo, D.; McLellan, H. M.; Imbrigiotta, T. E. Environ. Sci. Technol. 1997, 31 (12), 3565−3572.

(18) Butler, E. C.; Hayes, K. F. Water Res. 1998, 32 (5), 1345−1354.

(19) Ko, S. O.; Schlautman, M. A.; Carraway, E. R. Environ. Sci. Technol. 1998, 32 (18), 2769−2775.

(20) Jawitz, J. W.; Annable, M. D.; Rao, P. S. C.; Rhue, R. D. Environ. Sci. Technol. 1998, 32 (4), 523−530.

(21) Zimmerman, J. B.; Kibbey, T. C. G.; Cowell, M. A.; Hayes, K. F. Environ. Sci. Tech. 1999, 33 (1), 169−176.

(22) Allred, B.; Brown, G. O. Ground Water Monit. Rem. 1994, 14 (2), 174−184.

(23) Renshaw, C. E.; Zynda, G. D.; Fountain, J. C. Water Resour. Res. 1997, 33 (9), 371−378.

(24) Meegoda, N. J.; Rajapakse, R. A. ASCE J. Environ. Eng. 1993, 119 (4), 725−743.

(25) Tumeo, M. A. Ground Water Monit. Rem. 1997, 17 (4), 138−144.

(26) Harwell, J. H.; Schechter, R. S.; Wade, W. H. Soc. Petrol. Eng. J. 1984.

(27) Pankow, J. L.; Cherry, J. A. Dense Chlorinated Solvents and Other DNAPLs in Ground Water; Waterloo Press: Portland, OR, 1996.

(28) Moore, D. N.; Reynolds, R. C. J. X-ray Diffraction and the Identification and Analysis of Clay Minerals; Oxford University Press: New York, 1989.

(29) Ives, K. J.; Pienvichitr, V. Chem. Eng. Sci. 1965, 20, 965−973.

(30) Vandevivere, P.; Baveye, P.; del Lozada, S.; DeLeo, P. Water Resour. Res. 1995, 31 (9), 2173-2180.

(31) Karaborni, S.; Heidug, W.; Smit, B. Science 1996, 271, 1102−1104.

(32) Tien, C. Granular Filtration of Aerosols and Hydrosols; Butterworth: Boston, 1989.